Experimental Investigation of the Role of Fluid Turbulent Stresses and Edge Plasma Flows for Intrinsic Rotation Generation in DIII-D H-Mode Plasmas

S. H. Müller, J. A. Boedo, K. H. Burrell, J. S. deGrassie, R. A. Moyer, D. L. Rudakov, and W. M. Solomon

Experimental investigation of the role of fluid turbulent stresses and edge plasma flows for intrinsic rotation generation in DIII-D H-mode plasmas

S.H. Müller,[1,2] J.A. Boedo,[1] K.H. Burrell,[3] J.S. deGrassie,[3] R.A. Moyer,[1] D.L. Rudakov,[1] and W.M. Solomon[4]

[1] *Center for Energy Research, University of California of San Diego, 9500 Gilman Drive, M/C 0417, La Jolla, CA 92093, USA*
[2] *Center for Momentum Transport and Flow Organization*
[3] *General Atomics, PO Box 85608, San Diego, CA 92186-5608, USA*
[4] *Princeton Plasma Physics Laboratory, PO Box 451, Princeton, NJ 08543-0451, USA*
(Dated: January 25, 2011)

The first measurements of turbulent stresses and flows inside the separatrix of a tokamak H-mode plasma are reported, using a reciprocating multi-tip Langmuir probe at the DIII-D tokamak. A strong co-current rotation layer at the separatrix is found to precede intrinsic rotation development in the core. The measured fluid turbulent stresses transport toroidal momentum outward against the velocity gradient and thus try to sustain the edge layer. However, the inward transport of toroidal momentum leading to co-current core plasma rotation can only be explained by postulating the existence of large kinetic stresses, i.e. stresses originating in velocity space. Constraints from the evolution of both intrinsic and driven rotation profiles require the stresses to be independent of the local velocity and its gradient. The importance of such kinetic stresses is corroborated by the success of a simple orbit loss model, representing a purely kinetic mechanism, in the prediction of features of the edge co-rotation layer.

PACS numbers: 52.35.Ra, 52.55.Fa, 52.55.Dy, 52.25.Fi

Toroidal plasma rotation has a wide range of beneficial effects on stability, confinement and performance in tokamaks [1]. In addition to the driven rotation by tangential neutral beam injection (NBI), tokamak plasmas also exhibit rotation in the case of no apparent external momentum sources, which is referred to as *intrinsic* rotation. Due to both the practical relevance for magnetic confinement fusion and the broad general physics interest in systems that are apparently able to spontaneously change their rotation properties, intrinsic rotation has been extensively studied experimentally [2–8] and theoretically [9, 10]. Experiments have inferred an "intrinsic torque" located at the plasma edge [8, 11], and a role of scrape-off layer (SOL) flows as a source for toroidal rotation has been suggested [4]. Non-diffusive non-convective turbulent stresses (dubbed *residual stresses*) are strong candidates to explain the spin-up of the core plasma [9].

In this Letter, we report the first measurements of turbulent stresses and flows inside the last closed flux surface (separatrix) of a tokamak plasma in high-confinement mode (H-mode). The observation of a strong edge co-current rotation layer [4, 11] is found to precede the development of intrinsic core rotation. The measured fluid turbulent stresses transport momentum outward and thus try to sustain the edge layer, but strong kinetic stresses are required to explain the net inward transport of toroidal momentum from the layer into the core. Such strong kinetic stresses cannot be obtained within the established theory of (weakly) non-uniform fluids of Chapman and Enskog [12] and its application to magnetized plasmas by Braginskii [13], which break down in an H-mode pedestal since the macroscopic gradient scale lengths are of the order of the ion Larmor radius.

Recall the toroidal angular momentum balance equation for a magnetic field $\mathbf{B} = R^{-1}(I\hat{\boldsymbol{\varphi}} + \hat{\boldsymbol{\varphi}} \times \nabla\Psi) + \mathbf{B}^{\text{n.a.}}$ (R is the distance to the major axis, $\hat{\boldsymbol{\varphi}}$ is the toroidal unit vector, $-2\pi\Psi \equiv \int d^2\boldsymbol{\sigma} \cdot \mathbf{B}$ is the poloidal flux):

$$\partial_t(mR\Gamma_\varphi) + \nabla \cdot (R\Pi \cdot \hat{\boldsymbol{\varphi}}) - q(n\partial_t + \boldsymbol{\Gamma} \cdot \nabla)\Psi$$
$$-qR(nE_\varphi^{\text{n.a.}} + \hat{\boldsymbol{\varphi}} \cdot \boldsymbol{\Gamma} \times \mathbf{B}^{\text{n.a.}}) = R(C_\varphi + S_\varphi), \quad (1)$$

where $n \equiv \int d^3u\, f$, $\Gamma_i \equiv nv_i \equiv \int d^3u\, u_i f$, $\Pi_{ij} \equiv m\int d^3u\, u_i u_j f$, $C_\varphi \equiv m\int d^3u\, u_\varphi \mathcal{C}$ and $S_\varphi \equiv m\int d^3u\, u_\varphi \mathcal{S}$ are the moments of distribution function f, collision operator $\mathcal{C}$ and kinetic source $\mathcal{S}$ (u_i are the velocity space coordinates). The first three terms of Eq. (1) correspond to conservation of canonical angular momentum $mRu_\varphi - q\Psi$ in phase space. In absence of non-axisymmetric fields $E_\varphi^{\text{n.a.}} = 0$, $\mathbf{B}^{\text{n.a.}} = 0$, explicit sources $S_\varphi = 0$, in an equilibrium characterized by $\partial_t\Psi = 0$ and $\Gamma_\rho = 0$ ($\hat{\boldsymbol{\rho}} \equiv \nabla\Psi/|\nabla\Psi|$), and noting that $C_\varphi \propto -v_\varphi$ always opposes rotation, the only remaining candidate to explain an increase of ion angular momentum in a volume $V(\psi)$ is a finite stress at the boundary $\oint_{\partial V(\psi)} d^2\sigma\, R\Pi_{\varphi\rho} \neq 0$. The total stress can be written as $\Pi_{\varphi\rho} = mnv_\varphi v_\rho + \pi_{\varphi\rho}$, where $\pi_{\varphi\rho}$ represents kinetic stresses that cannot be expressed as functions of lower-order moments of f. Chapman-Enskog closure theory approximates π_{ij} in terms of the rate-of-strain tensor $W_{ij} \equiv \partial_i v_j + \partial_j v_i - \frac{2}{3}\partial_k v_k \delta_{ij}$, assuming a first-order expansion of f about a Maxwellian [12, 13]. Inherently, the estimates of $\pi_{\varphi\rho}$ are small, so that studies have focused on the $nv_\varphi v_\rho$ term [2, 9]. It is common to decompose all variables in time-average and fluctuating quantities, e.g. $A = \langle A \rangle + \tilde{A}$, and writing

$$\langle nv_\varphi v_\rho \rangle = \langle n \rangle\langle \tilde{v}_\varphi \tilde{v}_\rho \rangle + \langle v_\varphi \rangle\langle \tilde{n}\tilde{v}_\rho \rangle + \langle \tilde{n}\tilde{v}_\varphi \tilde{v}_\rho \rangle, \quad (2)$$

where $\langle v_\rho \rangle = 0$ is assumed and $\langle n \rangle\langle \tilde{v}_\varphi \tilde{v}_\rho \rangle$, $\langle v_\varphi \rangle\langle \tilde{n}\tilde{v}_\rho \rangle$ and
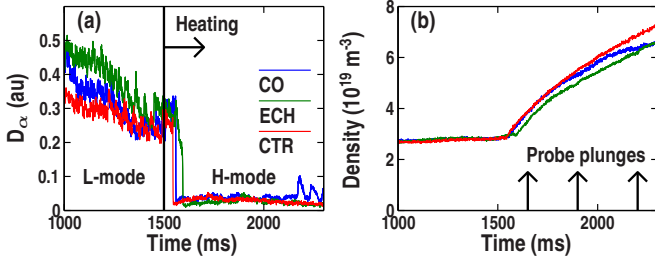
FIG. 1. (a) D_α signal as an indicator for L-H transition and ELM-freeness. (b) Line-integrated density evolution. The three probe plunges at different delays were performed in identical repeat shots and immediately followed by beam blips for a snapshot of the C^{6+} rotation profile.

$\langle \tilde{n}\tilde{v}_\varphi\tilde{v}_\rho \rangle$ are the contributions from Reynolds stress, particle transport and triple correlations, respectively.

In this Letter, using a reciprocating multi-tip Langmuir probe [11, 14], we present the first direct measurements of the terms in Eq. (2) in a tokamak H-mode pedestal. We use an arrangement of five probe tips (size 2 mm) [2] in the form of a tilted cross (distance between opposing tips 1 cm; tilt angle 30 degrees). Two pins, separated by a barrier (height 3 mm), are aligned along $\hat{\varphi}$ and measure the (mostly D^+) ion saturation fluxes $\Gamma_\pm$ (bias -300 V). A theory of ion collection by absorbing objects in combined parallel and perpendicular flows [15] is used to calculate the flow velocity in the direction of tip alignment and the unperturbed density: $v_\varphi = \frac{1}{2}c_s \ln(\Gamma_-/\Gamma_+)$; $n = [\exp(1)/c_s]\sqrt{\Gamma_-\Gamma_+}$. Note that the sound speed $c_s \equiv \sqrt{(T_e + T_i)/m_i} \approx \sqrt{2T_e/m_i}$ cancels in nv_φ. To compare $\langle n \rangle$ and $\langle v_\varphi \rangle$ against other diagnostics, $\langle T_e \rangle$ is measured on the central tip using a harmonics technique [16]. The two remaining, poloidally separated tips measure the floating potential difference δV, from which $\tilde{E}_\theta \approx -\delta\tilde{V}/\delta\ell$ and $\tilde{v}_\rho \simeq -\tilde{E}_\theta/B_\varphi$ are obtained, where $\hat{\theta} \equiv \hat{\rho} \times \hat{\varphi}$ and $\delta\ell$ is the poloidal separation. We use a sliding median filter of 0.5-ms width, corresponding to 1 mm of probe motion, to perform the background subtraction and a 2-ms sliding mean to calculate averages. Halving or doubling these choices does not significantly change the results. The results from all diagnostics, including the probe which is situated 18.8 cm below the midplane, were mapped to ψ using the EFIT equilibrium reconstruction code, resulting in good agreement between the probe and the Thomson scattering diagnostic for the n and T_e profiles. The probe does not perturb the discharge measurably by other diagnostics.

The reported experiment made use of the capability of DIII-D to produce edge localized mode (ELM)-free H-mode plasmas interchangeably with electron cyclotron heating (ECH) and co/counter current NBI, thereby altering the torque input while keeping the power input constant at about 1 MW. The ITER-like lower-single-null shape and base parameters of $B_{\varphi 0} = -1.6$ T, $I_p =$

1.3 MA and $n_0 = 3 \times 10^{19}$ m^{-3} were optimized for a reliable transition from low- to high-confinement mode (L-H transition) at the lowest possible powers and extremely long ELM-free characteristics (Fig. 1). All three heating schemes, turned on at 1500 ms, produced an L-H transition reliably at 1575 ± 25 ms, resulting in a prompt increase of the peaked core T_e profile and a slow, approximately linear increase of the flat core density profile. Beam fueling plays a negligible role in this density rise (Fig. 1). The probe plunges were timed to reach the dwell point, on a shot-to-shot basis, at 1650, 1900 and 2200 ms (NBI: 2300 ms). An earlier plunge was usually performed at 1000 ms for Ohmic and L-mode data. Approximately unperturbative diagnostic beam blips of 2-ms length were fired immediately after the dwell time to obtain snapshot profiles of the C^{6+} rotation. The main data set thus consists of a 3×3 matrix of different torques and delays in early ELM-free H-mode. Against our expectations, the n and T_e profiles in the lower half of the pedestal, which is accessible to the probe, were found *identical* for all 9 cases. With the gradients frozen, the pedestal height and width increase as the density rises.

Figure 2 shows the combined C^{6+} and D^+ rotation profiles, where we note that the impurity rotation is a good approximation for the main ion rotation in the core where gradients are weak, but not necessarily in the edge region [11]. The probe data shows clear evidence of a robust co-current rotation layer at the plasma edge. The layer is only 1 cm wide, peaks just inside the EFIT separatrix, and rotates co-current even when counter torque is applied to the core, although its magnitude decreases from 35 km/s to 25 km/s in this case. By the time of the earliest probe plunge 50 ms after the L-H transition, the layer has developed to its full size from a rudimentary feature in the Ohmic plasma 650 ms earlier. The lack of evolution over the following 650 ms in H-mode suggests that the L-H transition is the defining event for the rapid formation of the layer in our conditions. However, equally strong layers have been observed in different steady-state L-modes [11], indicating more complex conditions for layer formation.

In the ECH case with zero applied torque [Fig. 2(b,e)], intrinsic core rotation develops over a period of 600 ms after the first observation of the edge layer. The latest rotation measurement, peaking at 40 km/s, coincides in magnitude with the edge layer, but a dip in the rotation profile disproves a simple picture in which the core responds to a rotating boundary via viscous diffusion. A specific reanalysis of main-ion rotation data in similar helium plasmas [6], motivated by the Mach probe measurements, confirms both the existence of the edge co-rotation layer and the persistence of the dip during intrinsic rotation development. Application of co- and counter-NBI drive [Fig. 2(a,d) and 2(c,f)] has a strong impact on the velocity profile and its gradient, but the total resulting rotation appears well described as the sum
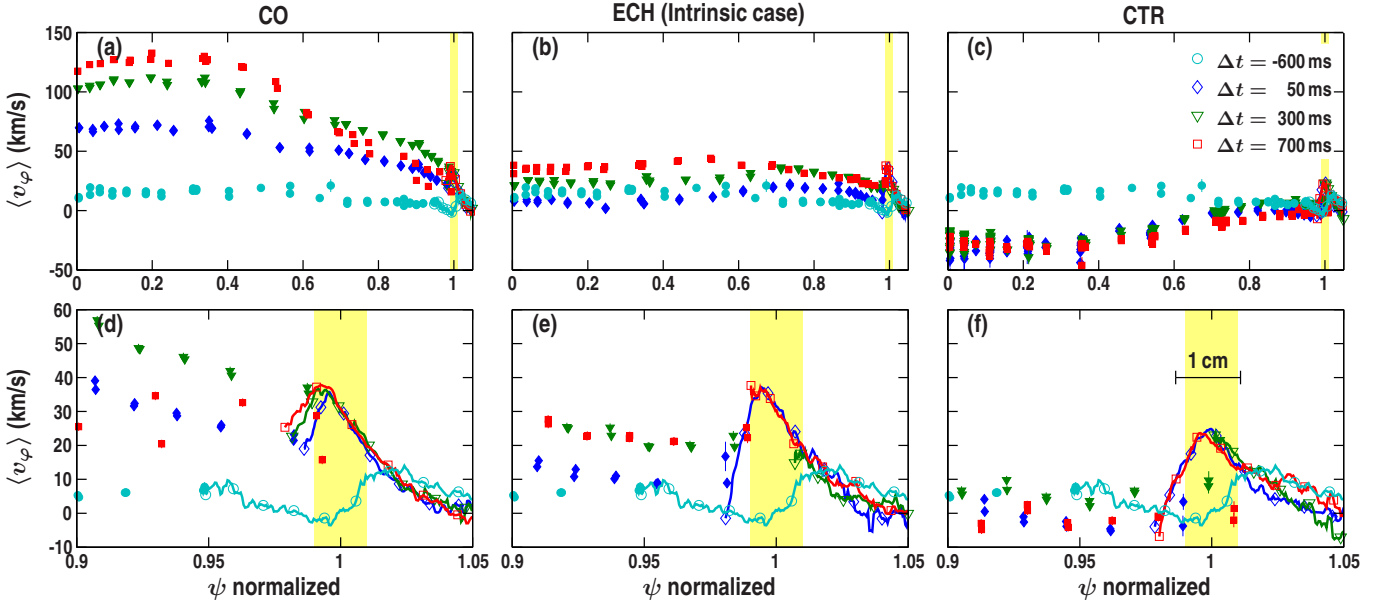
FIG. 2. (a-c) Combined C^{6+} (filled symbols) and probe (lines with open symbols) rotation profiles for different torque inputs and delays Δt after the L-H transition. An Ohmic profile is shown at $\Delta t = -600$ ms. Shaded areas indicate an estimated 95% confidence interval for the separatrix position. (d-f) Expanded view of the edge region. Error estimates are discussed in Fig. 4.
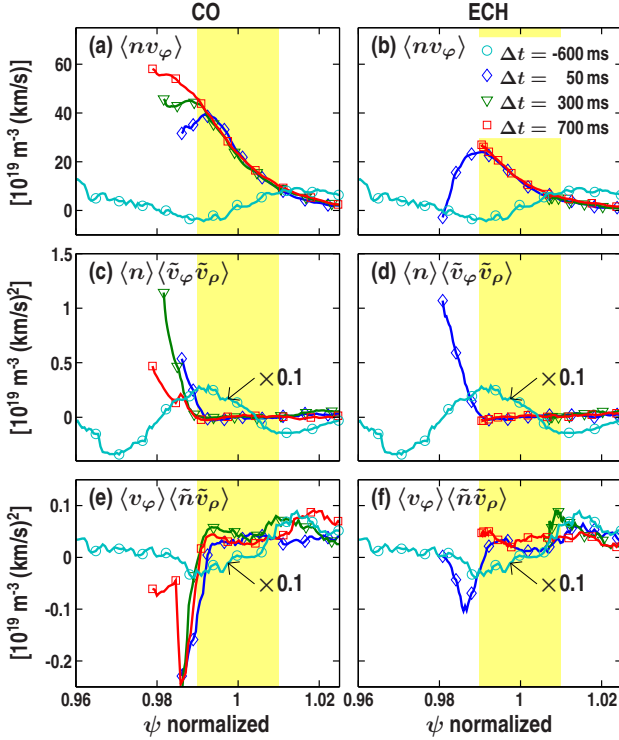

FIG. 3. Probe measurements of fluid turbulent stresses.

of a constant intrinsic part plus the beam-driven part, underlining the non-diffusive and non-convective nature of the stresses leading to intrinsic rotation.

The measured turbulence is broadband, ranging from 1 kHz to 1 MHz, with autocorrelation times of 2-20 μs.

The normalized fluctuation levels are low: $\langle \tilde{n}^2 \rangle^{1/2}/\langle n \rangle \sim \langle \delta \tilde{V}^2 \rangle^{1/2}/\langle T_e/e \rangle \sim \langle \tilde{v}_\varphi^2 \rangle^{1/2}/\langle c_s \rangle \sim 5\%$ for $\psi \lesssim 1$, increasing to about 30% at $\psi \simeq 1.03$. Absolute fluctuation levels and autocorrelation times exhibit a minimum at the peak of the edge co-rotation layer.

Figure 3 shows the toroidal momentum density $\langle n v_\varphi \rangle$ (a,b) of the edge layer and the measurements of the momentum transport terms in Eq. (2), $\langle n \rangle \langle \tilde{v}_\varphi \tilde{v}_\rho \rangle$ (c,d) and $\langle v_\varphi \rangle \langle \tilde{n} \tilde{v}_\rho \rangle$ (e,f) for the co-NBI and ECH cases. The contribution of triple correlations $\langle \tilde{n} \tilde{v}_\varphi \tilde{v}_\rho \rangle$ was generally found negligible. The particle transport contribution [Fig. 3(e,f)] becomes negative inside the peak of the layer, which is consistent with the global density rise (Fig. 1).

The Reynolds stress term $\langle n \rangle \langle \tilde{v}_\varphi \tilde{v}_\rho \rangle$ [Fig. 3(c,d)] is effectively zero outside the layer's peak and becomes increasingly positive further inward, dominating over the inward-directed term $\langle v_\varphi \rangle \langle \tilde{n} \tilde{v}_\rho \rangle$ in magnitude. It is neither proportional to $-\langle v_\varphi \rangle$ nor to $-\partial_\rho \langle v_\varphi \rangle$ and thus satisfies the definition of a *residual stress*, which acts to transport (positive) momentum outward, up the layer's inner flank, thus trying to sustain the co-rotation layer. However, this exerts a *counter-current* torque onto the core, which is clearly inconsistent with the fact that we see the core spinning up in the *co-current* direction.

Since the measured fluid turbulent stresses do not lead to a globally consistent picture, we revisit the possibility of kinetic stresses in the edge and estimate the required magnitudes from a global torque balance. Figure 4(a) shows the rate of change of cumulative angular momentum $L_\varphi(\psi) \equiv \int_{V(\psi)} d^3x \, m R n v_\varphi$, estimated from Thomson scattering and charge-exchange-
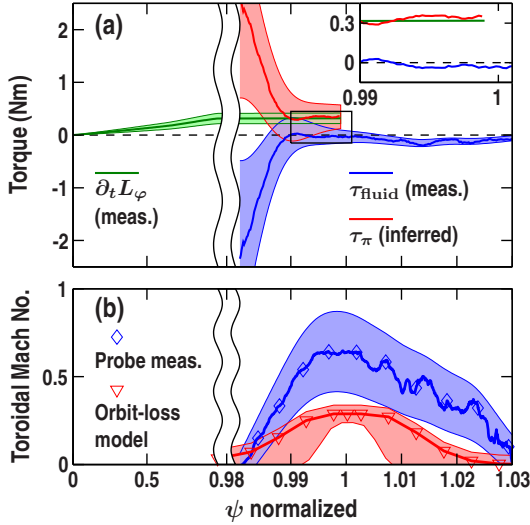
FIG. 4. (a) Torque balance for the ECH H-mode case at $\Delta t = 50\,\mathrm{ms}$. (b) A simple orbit loss model correctly predicts direction, location and width of the edge co-rotation layer. Shaded areas represent estimated 95% confidence intervals.

recombination spectroscopy. Under the present assumptions, this must be locally equal to the torque $\tau_\Pi(\psi) \equiv -\oint_{\partial V(\psi)} d^2\sigma\, R\langle\Pi_{\varphi\rho}\rangle$. The contribution from the measured fluid stresses, $\tau_{\mathrm{fluid}} \equiv -\oint_{\partial V(\psi)} d^2\sigma\, Rm\langle nv_\varphi v_\rho\rangle = -2\pi mL_{\mathrm{eff}}R^2\langle nv_\varphi v_\rho\rangle$, is also shown. Here, we assumed that the measurements are representative for an effective poloidal length of $L_{\mathrm{eff}} \sim 2\,\mathrm{m}$ on the low-field side and neglected contributions from the high-field side. Since $R^2\langle nv_\varphi v_\rho\rangle$ is most likely not a flux function, this assumption is subject to large uncertainties, which are factored into the error estimates in Fig. 4. For $\psi \simeq 0.98$, τ_{fluid} contributes -2 Nm of torque, which is opposite and much larger than the necessary +0.3 Nm that the core spin-up requires. It is thus necessary to infer a large torque $\tau_\pi \simeq +2.3\,\mathrm{Nm}$ from the kinetic stresses $\langle\pi_{\varphi\rho}\rangle$, about 20 times larger than what Chapman-Enskog theory would provide. For $\psi \sim 1$ at the layer's peak where the gradient is zero, $\tau_{\mathrm{fluid}} \simeq 0$ is measured (Fig. 4 inset), such that τ_π has to account for the full +0.3 Nm of torque. Taken together with the constraints from the rotation-profile evolution discussed earlier in Fig. 2, we must therefore require that the kinetic stresses $\langle\pi_{\varphi\rho}\rangle$ have the *same non-diffusive non-convective characteristics as a residual stress* everywhere in the interval $0.98 \leq \psi \leq 1$.

To give an example for a process that would lead to such kinetic stresses, results from a simple orbit loss model [7] are shown in Fig. 4(b). Conservation of canonical angular momentum along particle trajectories requires that co-moving ions drift inward, while counter-moving ones drift outward. In the vicinity of $\psi = 1$, this mechanism leads to a loss cone in velocity space, which alters the moments of f, including v_φ and $\Pi_{\varphi\rho}$. The model correctly predicts the existence, direction, position and

width of the edge co-rotation layer, while underestimating its magnitude by a factor of two. This highlights the necessity to include purely kinetic processes in the search for residual stresses in a tokamak H-mode pedestal and develop appropriate theory. Our results indicate that the decomposition $\Pi_{\varphi\rho} = mnv_\varphi v_\rho + \pi_{\varphi\rho}$ poorly reflects the nature of the present physical processes, suggesting the exploration of other venues.

In summary, we have presented the first measurements of fluid turbulent stresses and flows in a tokamak H-mode pedestal. The core rotation was observed to respond to the emergence of a strong edge co-current rotation layer, which appears to be at least partially created by purely kinetic processes. Full-f gyrokinetic codes that can treat the plasma edge [17] should be in a position to observe an edge co-rotation layer and confirm the existence of kinetic stresses that greatly surpass the Chapman-Enskog estimates in an H-mode pedestal. The smaller intrinsic rotation in L-mode in DIII-D could potentially be explained by an increased interaction of ion orbits with turbulence, leading to a symmetrization of the loss cone. The observed counter-current intrinsic rotation in L-mode in other devices [4, 5] may be related to other effects.

[1] K. H. Burrell, Phys. Plasmas **4**, 1499 (1997).

[2] C. Hidalgo *et al.*, Phys. Rev. Lett. **91**, 065001 (2003); B. Gonçalves *et al.*, Phys. Rev. Lett. **96**, 145001 (2006).

[3] J. E. Rice *et al.*, Nucl. Fusion **45**, 251 (2005); Plasma Phys. Control. Fusion **50**, 124042 (2008).

[4] B. LaBombard *et al.*, Phys. Plasmas **12**, 056111 (2005); Phys. Plasmas **15**, 056106 (2008).

[5] A. Bortolon *et al.*, Phys. Rev. Lett. **97**, 235003 (2006); R. A. Pitts *et al.*, J. Nucl. Mat. **363-365**, 505 (2007).

[6] J. S. deGrassie *et al.*, Phys. Plasmas **14**, 056115 (2007).

[7] J. S. deGrassie *et al.*, Nucl. Fusion **49**, 085020 (2009).

[8] W. M. Solomon *et al.*, Nucl. Fusion **49**, 085005 (2009).

[9] Ö. D. Gürcan *et al.*, Phys. Plasmas **14**, 042306 (2007); P. H. Diamond *et al.*, Nucl. Fusion **49**, 045002 (2009).

[10] Y. Camenen *et al.*, Phys. Rev. Lett. **102**, 125001 (2009).

[11] J. A. Boedo *et al.*, Phys. Plasmas (accepted) (2011).

[12] S. Chapman and T. G. Cowling, *The mathematical theory of non-uniform gases* (Cambridge University Press, Cambridge, England, 1953).

[13] S. I. Braginskii, *Reviews of Plasma Physics*, Vol. 1 (M. A. Leontovich, Consultants Bureau, NY, 1965) p. 205.

[14] R. A. Moyer *et al.*, Phys. Plasmas **2**, 2397 (1995).

[15] I. H. Hutchinson, Phys. Plasmas **15**, 123503 (2008).

[16] D. L. Rudakov *et al.*, Rev. Sci. Instrum. **72**, 453 (2001).

[17] C. S. Chang *et al.*, Phys. Plasmas **11**, 2649 (2004); C. S. Chang and S. Ku, Phys. Plasmas **15**, 062510 (2008).